Halogen Bonding Enhances Nonlinear Optical Response in Poled Supramolecular Polymers

Matti Virkki, Ossi Tuominen, Alessandra Forni, Marco Saccone,
Pierangelo Metrangolo, Giuseppe Resnati, Martti Kauranen and Arri Priimagi

February 12, 2015

Supplementary information

1 Sample fabrication

The synthesis of the Azo-X chromophores has been described earlier[1]. Thin-film samples of the polymer-azobenzene complexes were prepared by spin coating from DMF (P4VP) or from a 50/50 mixture of acetone/dichloroethane (PS). The chromophore concentrations used were 10 mol-% (P4VP) and 5 mol-% (both PS and P4VP). The samples are denoted as P4VP/PS(Azo-X)$_y$ where y stands for the number of azobenzenes per each polymer repeat unit (0.05 in PS; 0.05 or 0.1 in P4VP). All samples were homogeneous and amorphous as verified by optical microscopy. The sample thicknesses were measured using Dektak 150 surface profiler.

2 All-optical poling

The nonlinear optical response was studied using all-optical poling, a technique based on the polar orientational excitation of the chromophores [2, 3]. In our experiments, polar selectivity is reached due to interference between two-photon excitation at the fundamental 1064 nm wavelength and one-photon excitation at the seeding 532 nm wavelength that are present in the poling field. The poling process is periodically halted by blocking the seeding beam. During this time, the fundamental 1064 nm beam is still passed to the sample and the second-harmonic (SH) signal at 532 nm generated by the sample is measured using a photomultiplier tube. The poling light source is a mode-locked diode-pumped Nd:YAG laser with 1064 nm wavelength, 100 Hz repetition rate and 28 ps pulse length. The 532 nm seeding beam is produced by frequency-doubling a small portion of the fundamental beam using a DKDP crystal.

All-optical poling is highly sensitive to the relative phase and intensity between the fundamental (frequency ω) and seeding (frequency 2ω) fields. The optimal relative intensity, i.e. seeding ratio, is reached when the probability of two-photon absorption at the fundamental wavelengthis as high as the probability of single-photon absorption at the seeding wavelength. It has been shown that the optimum ratio can be written as [3]

$$\left|\frac{E_{2\omega}}{E_\omega^2}\right| = \frac{\Delta\mu}{2\sqrt{3}\hbar\omega} \tag{1}$$

where E_ω refers to the electric field at the fundamental frequency ω and $E_{2\omega}$ to the field at the seeding frequency 2ω and $\Delta\mu$ is the difference between the dipole moments in the ground and excited states of the chromophore molecules within the two-level approximation. The seeding ratio was optimized by fixing the fundamental beam power to 800 mW and performing the poling experiment with seeding beam powers ranging from 12.5 µW to 400 µW. The poling time for the lowest seed power was 25 minutes and for the highest seed power 5 minutes respectively. These times were chosen in order to let the second-harmonic response saturate during each measurement as the speed of the poling process increases with increasing seeding beam power.
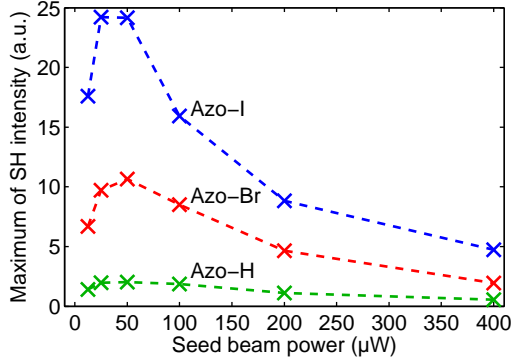
Figure S1: Second-harmonic (SH) intensities reached for different seeding ratios in all-optical poling for the studied chromophores in P4VP matrix. Dashed lines have been drawn to guide the eye.

While the exact phase difference between the fields is unknown, additional phase shift was introduced by rotating a 4 mm thick piece of BK7 glass in the beam line just before the sample. Four phase shifts $\Delta\Phi$ between 0 and $3\pi/4$ in $\pi/4$ steps were studied for each seeding ratio and sample separately. The second-harmonic signal from a thin film depends on the relative phase $\Delta\Phi$ as $1 + \cos(2\Delta\Phi)$ [3]. Therefore, one of our relative phases will show at least 85 % of the maximum second-harmonic signal even in the worst case that is found when the total phase difference is $\pi/8$ for zero additional phase shift.

The optimization results are shown in Fig. S1. The data points for a single sample represent the highest level of second-harmonic response that was reached in the phase optimization for each seeding beam power. The maximum second-harmonic intensity is reached at either 25 or 50 µW power for each sample. It is evident that the qualitative differences between the samples remain even when far away from the optimal seeding ratio. It is worthwhile to mention that according to Eq.1, in our experiments 25 µW seed power corresponds to $\sim$0.8$\times 10^{-10}$ m/V and 50 µW to $\sim$1.1$\times 10^{-10}$ m/V seeding ratio. These values are in excellent agreement with the optimum ratio of $\sim$0.9 $\times 10^{-10}$ m/V found for another azobenzene chromophore [3].

The extensive optimization measurements revealed that the same poling parameters are optimal for each of the studied chromophores. Therefore, the results presented in the main article have been acquired by using the seed power of 50 µW and additional phase of $\pi/2$ that were found to yield the highest second-harmonic responses.

3 Spectral characteristics

The photoinduced changes in the absorption spectrum were measured with a setup built around a multi-channel fiber spectrometer (AvaSpec-ULS2048L) with 0.6 nm resolution in the range of 175–1100 nm. The excitation source was a continuous-wave diode-pumped solid-state laser at 532 nm wavelength. Circular polarization was used in order to avoid photoinduced rearrangement of the chromophores. The excitation beam was expanded to about 20 mm diameter and cut to 6 mm using an iris in order to achieve a top-hat profile and equally efficient photoactivation in the whole studied sample area. The excitation beam power reaching the sample was adjusted to 5.65 mW which leads to 20 mW/cm^2 intensity. For the white light probe beam, a balanced deuterium halogen light source (AvaLight-HD-S-BAL) was used. The probe beam power was adjusted to less than 0.1 mW and its diameter was 4.6 mm at the sample. The small peak found at 486 nm in some of the absorption spectra can be attributed to the strong emission line of deuterium at this wavelength together with slight nonlinearity of the spectrometer.

A single spectral measurement was averaged over a 1.1 second interval. The spectrum was first measured just before the excitation light was focused on the sample. The excitation time was 5 s and the second measurement was carried out 10 s after the excitation was ended. The following measurements were carried out after 1, 3, 10, 30, 90 and 180 minutes after the excitation was ended. The absorption spectra measured are shown in Fig. S2. The wavelength and absorbance at the peak near 450 nm were found by fitting a second-order polynomial to 41 data points nearest to the maximum value found in the range 400–500

Table S1: Spectral characteristics and thicknesses of 5 mol-% samples. λ_{peak}: Wavelength of lowest energy peak in absorbance, A_{peak}: absorbance at λ_{peak}, ΔA_{peak}: relative change in absorbance after 532 nm excitation, A_{532}: absorbance at 532 nm, d: thickness

| material	P4VP(Azo-I)	P4VP(Azo-Br)	P4VP(Azo-H)	PS(Azo-I)	PS(Azo-Br)	PS(Azo-H)
λ_{peak} (nm)	462	463	449	449	445	435
A_{peak}	0.5668	0.5560	0.6600	0.8511	0.8163	0.8780
ΔA_{peak} (%)	23	20	18	21	19	14
A_{532}	0.2061	0.2111	0.1522	0.1674	0.1529	0.0996
d (nm)	470	480	570	900	700	740

nm. The fitting was done as measurement noise could cause a few nanometer errors in the locations of the spectral peaks due to the broad nature of the lowest energy peak found with azobenzene molecules. The largest difference between the fitting result and the data point with highest absorbance was 3 nm. For the isosbestic points the sum of least square deviations from the average value was calculated for each wavelength in the range of 350–450 nm and the minimum was chosen.

The absorption spectra of the 5 mol-% P4VP(Azo-X) and PS(Axo-X) samples are shown in Fig. S2 and the essential data is gathered to table S1. The photoexcitation experiments reveal that efficient isomerization is achieved for each material system. In each case, a notable drop in absorbance is found near the 450 nm peak accompanied with an increase in the range 350–400 nm. Such a change is characteristic for azobenzene derivatives as they isomerize into the *cis* form [4]. The isosbestic points (marked with dashed lines) were found in the range 389–401 nm following the order of the locations of the absorbance peaks. The time series reveals that thermal relaxation of the *cis* isomer back to the thermally stable *trans* isomer is rather slow in the studied systems, particularly in the PS matrix but the differences between chromophores are small. Furthermore, some of the samples were studied approximately 22 h after excitation and the absorption spectrum was found to regain the dark-adapted profile in this time frame proving that no permanent changes occur at the molecular level.
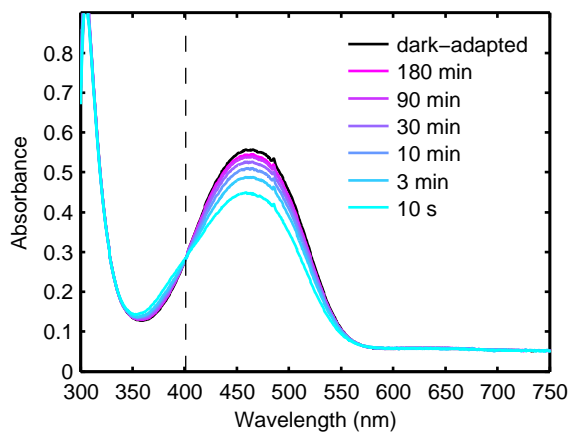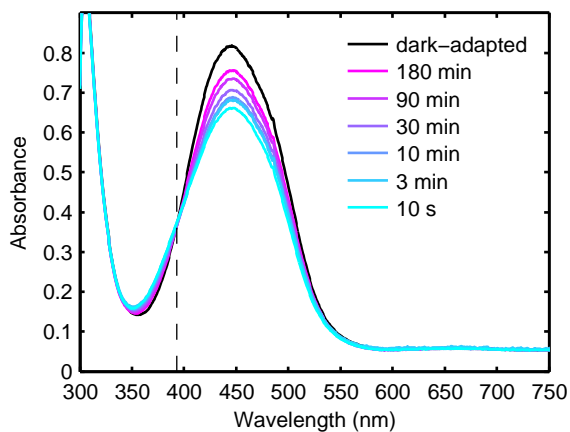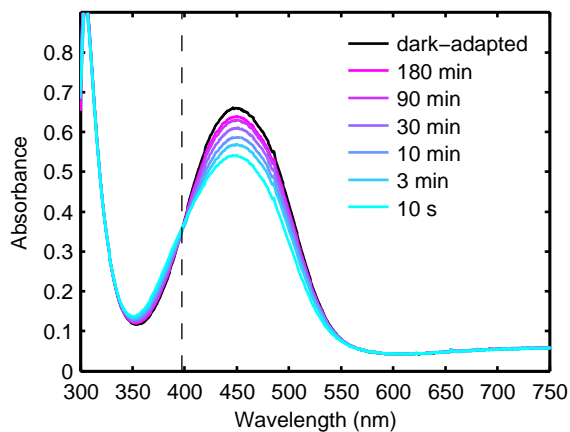
(a) P4VP(Azo-I)$_{0.05}$
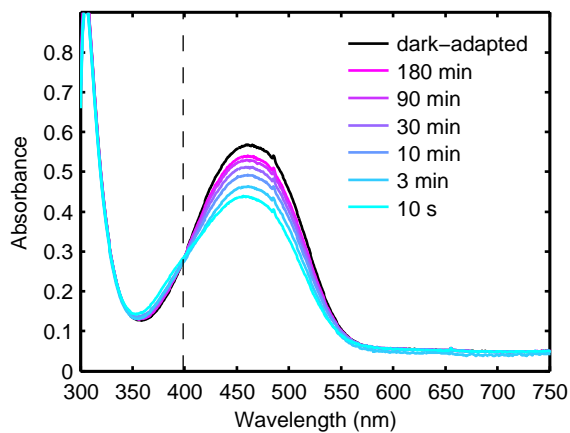
(b) PS(Azo-I)$_{0.05}$
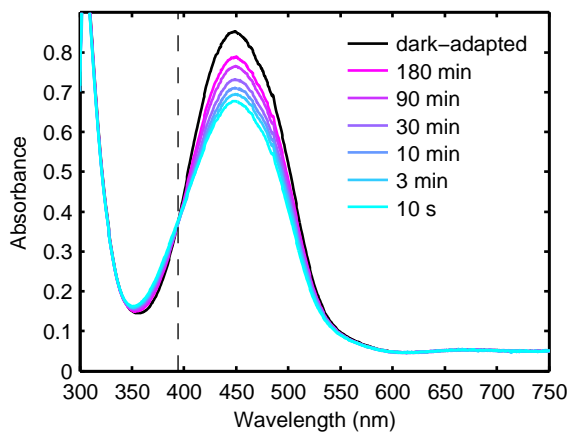
(c) P4VP(Azo-Br)$_{0.05}$

(d) PS(Azo-Br)$_{0.05}$
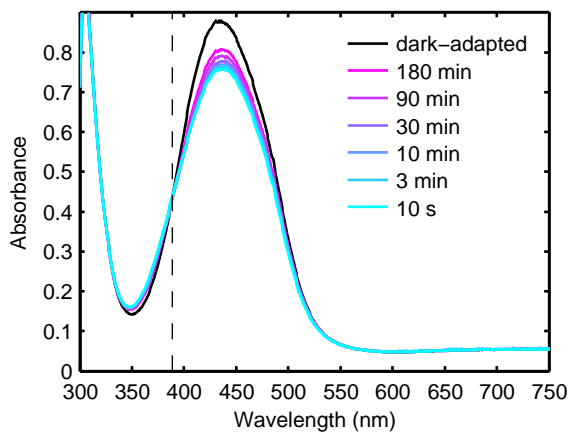
(e) P4VP(Azo-H)$_{0.05}$

(f) PS(Azo-H)$_{0.05}$

Figure S2: Spectral changes in 5 mol-% Azo-X samples before and after 5 s excitation at 20 mW cm^{-1} 532 nm.

4

4   Birefringence with 532 nm excitation

Photoinduced birefringence was achieved by directing a vertically polarized beam from a continuous-wave diode-pumped solid-state laser at 532 nm wavelength with 16 mW/cm^2 intensity onto the samples. The induced birefringence due to orientation-dependent photoexcitation and following angular redistribution was studied in real-time with a probe beam at 780 nm. The probe beam was directed onto the sample through a polarizer at +45° angle with respect to the excitation beam polarization. After the sample, the beam was directed onto a photodiode through an analyzing polarizer at -45° angle. Such a setup allows the intensity I measured with the photodiode to be connected to the absolute difference in refractive index $|\Delta n|$ by [5]

$$I = I_0 \sin^2\left(\frac{\pi|\Delta n|l}{\lambda}\right), \tag{2}$$

where I_0 is the reference intensity measured with the polarizer and analyzer parallel, l is the thickness of the sample and λ is the wavelength of the probe beam. The time evolution of the photoinduced birefringence in 5 mol-% Azo-X samples is shown in Fig. S3.
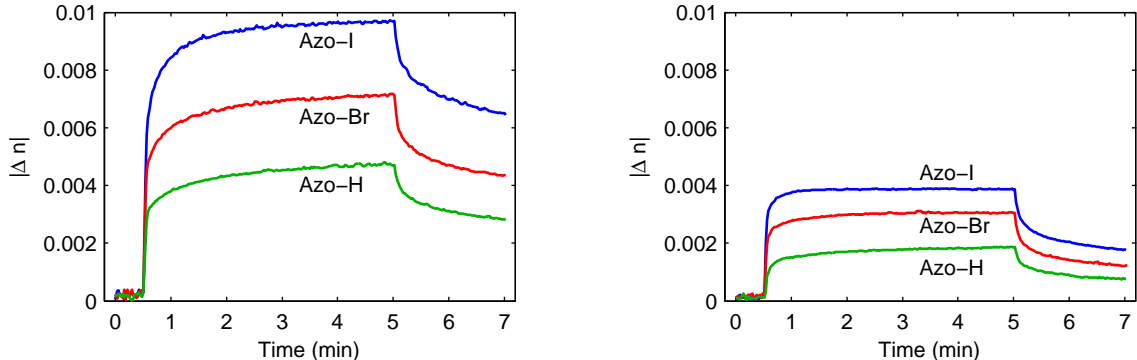

Figure S3: Photoinduced birefringence of 5 mol-% Azo-X samples in P4VP matrix (left) and PS matrix (right).

The birefringences follow the qualitative order (I > Br > H and P4VP > PS) presented in the main article for second-harmonic generation but quantitative differences are notably smaller.

5   Computational methods and additional theoretical results

The molecular dimers of compounds Azo-X with either 4-methylpyridine or methylbenzene were optimized at the M062X/6-311++G** level of theory *in vacuo*. The basis set for iodine[6] was downloaded from the Basis Set Exchange site.[7, 8] The M062X functional has been chosen in view of its optimal performance in treating noncovalent interactions,[9] including in particular halogen bonding with both lone pairs of heteroatoms[10] and π electron systems.[11] Interaction energies have been computed by optimization on the BSSE-free potential energy surface as the difference between the energy of the dimer and the sum of the energies of the single monomers. BSSE correction was made by the standard counterpoise method.[12] All calculations were performed with the Gaussian suite of programs.[13]

Molecular hyperpolarizabilities and dipole moments of the Azo-X chromophores are shown in table S2. Hyperpolarizabilities were obtained with the coupled-perturbed Kohn-Sham method at 1064 nm wavelength. The (99,590) grid, referred to as the ultrafine grid in Gaussian09, has been used for the DFT numerical integrations.

Table S2: M062X/6-311++G(d,p) computed dipoles and hyperpolarizabilities along the dipole direction of the Azo-X series.

Compound	μ(D)	$\beta_z(\times 10^{-30})$esu
Azo-I	6.72	271
Azo-Br	6.90	296
Azo-H	5.87	225

References

[1] A. Priimagi, G. Cavallo, A. Forni, M. Gorynsztejn-Leben, M. Kaivola, P. Metrangolo, R. Milani, A. Shishido, T. Pilati, G. Resnati, and G. Terraneo, "Halogen Bonding versus Hydrogen Bonding in Driving Self-Assembly and Performance of Light-Responsive Supramolecular Polymers," Adv. Funct. Mater. **22**, 2572 (2012).

[2] N. B. Baranova and B. Y. Zel'dovich, "Physical effects in optical fields with nonzero average cube, $< E >^3 \neq 0$," J. Opt. Soc. Am. B **8**, 27 (1991).

[3] C. Fiorini, F. Charra, J. M. Nunzi, and P. Raimond, "Quasi-permanent all-optical encoding of noncentrosymmetry in azo-dye polymers," J. Opt. Soc. Am. B **14**, 1984 (1997).

[4] Z. Sekkat and W. Knoll, *Photoreactive organic thin films*, Academic Press, San Diego (2002).

[5] T. Todorov, L. Nikolova, and N. Tomova, "Polarization holography. 1: A new high-efficiency organic material with reversible photoinduced birefringence," Appl. Opt. **23**, 4309 (1984).

[6] M. N. Glukhovtsev, A. Pross, M. P. McGrath, and L. Radom, "Extension of Gaussian-2 (G2) theory to bromine- and iodine-containing molecules: Use of effective core potentials," J. Chem. Phys. **103**, 1878 (1995).

[7] D. Feller, "The role of databases in support of computational chemistry calculations," J. Comput. Chem. **17**, 1571 (1996).

[8] K. L. Schuchardt, B. T. Didier, T. Elsethagen, L. Sun, V. Gurumoorthi, J. Chase, J. Li, and T. L. Windus, "Basis Set Exchange: A Community Database for Computational Sciences," J. Chem. Inf. Model. **47**, 1045, pMID: 17428029 (2007).

[9] Y. Zhao and D. Truhlar, "The M06 suite of density functionals for main group thermochemistry, thermochemical kinetics, noncovalent interactions, excited states, and transition elements: two new functionals and systematic testing of four M06-class functionals and 12 other functionals," Theor. Chem. Acc. **120**, 215 (2008).

[10] S. Kozuch and J. M. L. Martin, "Halogen Bonds: Benchmarks and Theoretical Analysis," J. Chem. Theory Comput. **9**, 1918 (2013).

[11] A. Forni, S. Pieraccini, S. Rendine, and M. Sironi, "Halogen bonds with benzene: An assessment of DFT functionals," J. Comput. Chem. **35**, 386 (2014).

[12] S. F. Boys and F. d. Bernardi, "The calculation of small molecular interactions by the differences of separate total energies. Some procedures with reduced errors," Mol. Phys. **19**, 553 (1970).

[13] M. J. Frisch, G. W. Trucks, H. B. Schlegel, G. E. Scuseria, M. A. Robb, J. R. Cheeseman, G. Scalmani, V. Barone, B. Mennucci, G. A. Petersson, H. Nakatsuji, M. Caricato, X. Li, H. P. Hratchian, A. F. Izmaylov, J. Bloino, G. Zheng, J. L. Sonnenberg, M. Hada, M. Ehara, K. Toyota, R. Fukuda, J. Hasegawa, M. Ishida, T. Nakajima, Y. Honda, O. Kitao, H. Nakai, T. Vreven, J. A. Montgomery, Jr., J. E. Peralta, F. Ogliaro, M. Bearpark, J. J. Heyd, E. Brothers, K. N. Kudin, V. N. Staroverov, R. Kobayashi, J. Normand, K. Raghavachari, A. Rendell, J. C. Burant, S. S. Iyengar, J. Tomasi, M. Cossi, N. Rega, J. M.

Millam, M. Klene, J. E. Knox, J. B. Cross, V. Bakken, C. Adamo, J. Jaramillo, R. Gomperts, R. E. Stratmann, O. Yazyev, A. J. Austin, R. Cammi, C. Pomelli, J. W. Ochterski, R. L. Martin, K. Morokuma, V. G. Zakrzewski, G. A. Voth, P. Salvador, J. J. Dannenberg, S. Dapprich, A. D. Daniels, . Farkas, J. B. Foresman, J. V. Ortiz, J. Cioslowski, and D. J. Fox, "Gaussian 09 Revision D.01," Gaussian Inc. Wallingford CT 2013.